

## **Massive influence of Himalayan source on sedimentation along northern Indian peninsular basin**

**A. Peketi\*<sup>1</sup>, A. Mazumdar<sup>1</sup>, B. Sawant<sup>1,2</sup>, S.P.K. Pillutla<sup>1,3</sup>, Subhashree Mishra<sup>1</sup>**

<sup>1</sup>CSIR- National Institute of Oceanography, Dona Paula, Goa-403004, India.

<sup>2</sup>Government College of Arts, Science and Commerce, Sanquelim, Goa. 403505, India.

<sup>3</sup>School of earth, ocean, and atmospheric sciences, Goa University, Taleigao, Goa 403206, India.

\*Corresponding author: aditya@nio.org

### **Abstract**

A 30 m long sediment core (MD161-19) spanning 320 ka, collected from the intermediate water depths of (1480 m) of Mahanadi offshore was subjected to provenance analyses using Sr and Nd isotope systematics. The Sr-Nd isotope ratios of MD161-19 fall on the mixing line defined by Ganga and Brahmaputra main stem averages. Strontium and Nd isotope ratios along with Fe/Al ratio clearly show the predominance of Himalayan sediments in the study area. The significant temporal variations in the Sr-Nd isotope ratios observed for the entire depositional age (320 ka) may be attributed to changes in the relative sediment contribution by Ganga and Brahmaputra river systems draining terrains with contrasting Sr-Nd isotope ratios. The temporal geochemical profiles coupled with precipitation profile show that wet-phases during stadials led to enhanced erosion of the trans-Himalayan batholiths (THB) rocks (characterized by high  $\epsilon_{Nd}$  values) possibly due to glacial expansion in the higher reaches of the Brahmaputra catchment. The warm interstadials coupled with enhanced precipitation are accompanied by a shift towards lower  $\epsilon_{Nd}$  values which may be attributed to extensive erosion of the Ganga catchment area comprising rocks characterized by lower  $\epsilon_{Nd}$  values and diminished THB contribution due to lack of glacial influence.

**Keywords:** Ganga, Brahmaputra, Himalayas, sediment provenance, peninsular India, Mahanadi basin.

### **Highlights**

- Bengal fan controls the sedimentation of the peninsular Indian (Mahanadi) basin.
- Sr-Nd isotope ratio variations show variable sediment flux of Ganga and Brahmaputra rivers.
- Climatic forcings controls the composition of the Bengal fan sediments.

## Introduction

The Bay of Bengal (BoB) is one of the major sinks of sediments derived from diverse sources that include the Himalayas, Trans-Himalayan plutonic belt (TPB), Indo Burman ranges, peninsular cratonic regions and large igneous province (LIP) such as Deccan Traps (Fig. 1). The major rivers draining the Indian sub-continent play a vital role in the accumulation of ~1350 million tons of sediments annually into the BoB (Milliman and Syvitski, 1992). The Ganga and the Brahmaputra rivers drain the entire central part of the Himalayan range and deliver  $\sim 1,060 \times 10^6$  Mt of sediments annually, 90% of which is deposited during monsoon seasons in the BoB (Subramanian, 1996). The peninsular rivers such as Krishna, Godavari, and Mahanadi deliver relatively less continental detritus compared to the Ganga-Brahmaputra river systems to the BoB (Chakrapani & Subramanian, 1990; Milliman and Syvitski, 1992).

The sediments transported by the Ganga-Brahmaputra river system to the BoB have been extensively studied (Galy et al., 1999; Pierson-Wickmann et al., 2001; Singh et al., 2007, 2008; Clift et al., 2008; Garzanti et al., 2011, Lupker et al., 2013; Peketi et al., 2021). However, the sediments deposited at the peninsular margins of the Bay of Bengal have received much less attention. Tripathy et al. (2011) studied the Sr-Nd isotopic composition and elemental geochemistry of sediments from the deep abyssal plain off Krishna–Godavari Basin and reported decreased contribution of sediments from the Himalayas during last glacial maximum (LGM) due to the weakening of SW monsoon and extension of glacial cover (Owen et al., 2002). Peketi et al. (2021) by means of Sr-Nd isotope ratios reported the predominant influence of Bengal fan sedimentation in the deep water end of the Mahanadi basin (water depth:  $\sim 2513$  m). Similarly, Dangwal et al. (2008) based on geophysical studies, reported a predominance of Himalayan sediments in the deep waters of the Mahanadi basin. However, there is a paucity of information on the sediments deposited at the shallow peninsular regions of BoB, where the influence of peninsular rivers like Mahanadi on the composition of sediments could be significant as compared to the deeper regions of the Bay. Phillips et al. (2014) utilized a multi-proxy approach to constrain the source of lithogenic components during the last 110 ky in the core off Mahanadi Basin and concluded that the terrigenous sedimentation in Mahanadi basin is primarily controlled by the monsoon intensity variation. The study (Phillips et al., 2014) considered terrigenous sediments in the Mahanadi basin are fed by peninsular Indian lithologies. Mazumdar et al. (2015) studied the elemental composition of Mahanadi basin sediments and discussed the contribution of Archean Proterozoic Granitic Gneiss (APGC) source rocks in the Mahanadi basin. Apart from these few works, the peninsular margin of BoB is relatively under-studied.

In this study, we have used high-resolution Sr-Nd isotope and Fe/Al concentration ratios coupled with grain size distribution data of MD161-19, retrieved from the offshore Mahanadi Basin (Fig.1) spanning 320 ka (up to MIS-8; Da Silva et al., 2017) to decipher the sediment sources and the role of climate on the sediment composition.

## **Geology**

Mahanadi basin is one of the major sedimentary basins of India. The basin is located along the east coast of India and formed due to rifting of Gondwanaland during Jurassic period (Sastri et al., 1981; Subrahmanyam et al., 2008). The basin extends both on onshore (1,41,589 km<sup>2</sup>; Subrahmanyam et al., 2008) and offshore (2,60,000 km<sup>2</sup>; Singh, 2008) with water depth exceeding 3000 m (Singh, 2008). Mahanadi river is the major sediment carrier to the Mahanadi basin. Sedimentation in the deeper water end (water depth: ~2500 m) of the Mahanadi basin is controlled by Himalayan sediments (Dangwal et al., 2008; Peketi et al., 2021). The annual sediment load of Mahanadi river is  $17.4 \pm 12.7 * 10^6$  tons (Bastia and Equeenuddin, 2016). The Mahanadi river is 850 km long and drains over major lithologies like Eastern Ghats (56 %), sedimentary rocks of Gondwana age (39 %) and recent alluvium/littoral deposits (5 %; Chakrapani and Subramanian, 1990; Meert et al., 2010). The Eastern Ghats are characterised by Late Archaean and early Proterozoic granite batholiths, tonalite-trondjhemite gneisses (TTGs), and charnockites and khondalites, whereas sedimentary rocks are consisting of limestone, shale and sandstone.

## **Methodology**

A sediment core (MD161-19; 39 m long) off Mahanadi Basin (Lat.:18°59.10' N; Long.:85°41.16' E) was retrieved with a giant Calypso piston corer onboard ORV Marion Dufresne (MD161) at a water depth of 1480 m. The sediment core was collected using a PVC liner of 10 cm inner diameter. The sediment core was sub-sampled at an interval of 5 cm for solid phase analysis. An aliquot of the sediment sample was freeze-dried and homogenized using agate mortar & pestle and stored in closed containers. The sediment samples were made carbonate-free using 0.6 N HCL (Peketi et al., 2020). The samples were later washed with ultrapure water, dried, homogenized, and subsequently combusted in a muffle furnace at 550<sup>0</sup> C for 4 hours to oxidize organic matter. A known weight of the sample (~50mg) was digested in acid-washed Savillex PTFE containers and brought to a completely clear solution using a standard acid mixture (HF-HNO<sub>3</sub>-HCl) following Peketi et al. (2021). Elemental concentrations of lithogenic fraction were determined by using Quadrupole ICP-MS (Thermo Scientific iCAP Q) using Rh as an internal standard (Peketi et al., 2020; 2021). MAG-1 was used as a standard material for checking the accuracy and reproducibility of the analysis. The

measured elemental concentrations for MAG-1 are within the reported values. Analytical precision was maintained by running several samples digested from the same aliquot of sediment. RSD for the measured elements was less than 3%.

Sr and Nd isotope ratio measurements were also made on the silicate fraction of the sediments. The sediments are brought to a completely clear solution in a Savillex container by HF-HNO<sub>3</sub> acid digestion following Peketi et al, (2020). Sr and Nd were separated from the solution using standard ion exchange procedures. Cation exchange columns filled with Eichrom 50X-8 resin were used for the concentration and separation of Sr and rare earth elements (REE). Separation of Nd from other REEs was done using Eichrom Ln-specific resin with 0.27 N HCl as an eluent. Sr-Nd isotopic ratio measurement was carried out using MC-ICP-MS (NU Plasma III). No blank corrections were applied to both Sr and Nd ratios since the signal of the procedural blank was significantly lower (>10<sup>3</sup> orders of magnitude) than the samples. Mass fractionation corrections for Sr and Nd were made by normalizing <sup>86</sup>Sr/<sup>88</sup>Sr to 0.1194 and <sup>146</sup>Nd/<sup>144</sup>Nd to 0.7219. During the course of the analysis, SRM-987 and JNdi-1 were repeatedly analyzed and monitored. The yielded values for both standards are within the recommended range of values. The <sup>143</sup>Nd/<sup>144</sup>Nd ratios of the sediments are normalized with CHUR (Chondritic Uniform Reservoir) and represented as εNd.

The grain size distribution of the sediments was determined by using a Microtrac S3500 laser particle size analyzer. Freeze-dried sediment samples were desalinated, decarbonated (1N HCl) and H<sub>2</sub>O<sub>2</sub> treated for removal of sea salts, carbonates, and organic matter respectively. The samples dispersed in water were decoagulated before introducing into the sample dispersion cell and later measured with the help of the auto sequence function provided by Microtrac.

## Results

The Sr and Nd concentrations vary from 49.0 to 171.1 and 18.3 to 43.2 ppm respectively, whereas, the <sup>87</sup>Sr/<sup>86</sup>Sr ratios and εNd values range from 0.72011 to 0.74893 and -18.4 to -12.2 respectively (Table 1). The data points on the <sup>87</sup>Sr/<sup>86</sup>Sr vs εNd scatter plots fall on the Ganga and Brahmaputra river sediment's mixing curve (blue dashed line; Fig. 2). Strontium and Nd isotope ratios show significant temporal variations across MIS-1 to MIS-8 (Fig. 3). Oxygen isotope ratios of *G.ruber* (δ<sup>18</sup>O<sub>*G.ruber*</sub>) was also incorporated along with the Sr-Nd isotope ratios to delineate the marine isotope ratios (Fig. 3). During the stadials, Nd isotope ratios show an overall negative correlation with the precipitation profile for the last 320 ka (Fig. 4). During wet periods of stadials, εNd values are more close to the main stem average of Brahmaputra (marked with black arrows; Fig. 4). During interstadials, the εNd values are more towards the main stem average of Ganga river bed sediments. Iron and Al contents vary from 3.2

to 6.2 (wt. %) and 5.9 to 10.9 (wt. %) respectively (Table 1). The Fe/Al ratios of lithogenic fraction vary from 0.5 to 0.7 (Fig. 5). The data cluster on the Fe/Al vs  $\epsilon$ Nd scatter plot lies within ranges for Ganga and Brahmaputra river sediments (Fig. 5). Sediment grain analyses suggest clay content ranging from 9.7 to 50.3 % (Table 1). The sediment core extends up to ~ 3,00,000 years and eight Marine Isotope Stages (MIS 1-8; Fig. 3) representing interglacial and glacial changes are demarcated using  $\delta^{18}\text{O}_{\text{G. ruber}}$  profile (Da Silva et al., 2017).

## Discussion

### Sediment provenance

To understand the sediment provenance, the  $^{87}\text{Sr}/^{86}\text{Sr}$  and  $\epsilon$ Nd values were plotted on mixing curves having the end members higher Himalayas (HH), lesser Himalayas LH, APGC, and DcB (Fig. 2). Apart from these end members, mainstem averages ( $^{87}\text{Sr}/^{86}\text{Sr}$  and  $\epsilon$ Nd) of Ganga, Brahmaputra rivers (Goodbred et al., 2014; Singh & Lanord, 2002; Singh et al., 2008), Godavari (Ahmad et al., 2009), Krishna (Ahmad et al., 2009), Mahanadi (Peketi et al., 2021) river bed sediments are also included. The  $^{87}\text{Sr}/^{86}\text{Sr}$  and  $\epsilon$ Nd values of the studied core fall on the mixing line (blue dashed line) of the mainstem average  $^{87}\text{Sr}/^{86}\text{Sr}$  and  $\epsilon$ Nd values of Ganga and Brahmaputra rivers and fall far away from the Mahanadi river bed sediments (Fig. 2). The Sr-Nd isotope ratios of the present study overlap with that of sediments recovered from the upper, middle, and lower Bengal fans (Fig. 2). In other words, the Sr-Nd isotope ratios show the predominance of Himalayan sediments and possibly less significant contribution from Mahanadi river system. Although the studied core was retrieved from the Mahanadi basin, the distribution of the Sr-Nd isotope ratios falls far from the Mahanadi river bed sediments (Fig. 2) and does not show any signatures of the significant contribution from the major lithologies in the Mahanadi basin such as Archean Proterozoic granitic genesis and Proterozoic sediments of Chattisgarh basin (George and Ray, 2020). This may be possible because of the large sediment deposition by the Ganga-Brahmaputra river system ( $\sim 1060 \times 10^6$  tons/year; Milliman and Syvitski, 1992) when compared to that of the Mahanadi river ( $17.4 \pm 12.7 \times 10^6$  tons/year; Bastia and Equeenuddin, 2016). The predominance of Himalayan sediments in the deep waters ( $\sim 2513$  m) of the Mahanadi basin has recently been reported by Peketi et al, (2021). Few data points falling on the mixing line of APGC and DcB (Fig. 2) show the signature of sediments derived by mixing of sediments from Deccan Basalts (70-80 %) and Archean Proterozoic gneissic complexes (20-30 %). However, this possibility can be negated as the Mahanadi river drainage area does not comprise Deccan basalts (Chakrapani and Subramanian, 1990). For further understanding, Fe/Al and  $\epsilon$ Nd data of the studied core was cross-plotted (Fig. 5) along with the data of Deccan Basalts, Archean Proterozoic gneissic

complexes source rocks, Ganga, and Brahmaputra river sediments (Subramanian et al., 1985; Singh & France-Lanord, 2002; Singh et al., 2005; Singh, 2009). The data cluster of the present studied core falls (Fig. 5) well within the ranges of Ganga and Brahmaputra river bed sediments. This further supports the predominance of Ganga-Brahmaputra derived sediments in the study area. The absence of the correlation between the  $^{87}\text{Sr}/^{86}\text{Sr}$  ratios and the median grain size ( $D_{50}$ ) (Fig. 6) indicates lack of grain size effect (clay) on the  $^{87}\text{Sr}/^{86}\text{Sr}$  ratios during the studied time period.

### **Role of climatic condition on Sr-Nd temporal variations**

The  $^{87}\text{Sr}/^{86}\text{Sr}$  and  $\epsilon\text{Nd}$  ratios show marked temporal variations throughout the time span of 320 ky BP (Fig. 3) which may be attributed to change in the relative contribution from the Ganga and Brahmaputra river sediments with contrasting Sr-Nd isotopic compositions (Goodbred et al., 2014; Singh & Lanord, 2002; Singh et al., 2008). Climatically driven changes in the relative sediment contribution by Ganga and Brahmaputra have earlier been documented from sediment cores collected from Bengal fan (Galy et al., 2010; Hein et al., 2017) and deeper waters of the east coast of India (Peketi et al., 2021). To address the influence of climatic changes on the temporal variations in Sr-Nd isotope ratios, we have used the precipitation profile ( $\delta^{18}\text{O}_{\text{sw}}$ ) of the last 320 ky generated from an IODP-353 core U1446 (Clemens et al., 2021) close to our study area and  $\delta^{18}\text{O}_{\text{G.rubber}}$  profile of MD161-19 (Da Silva et al., 2017). A correlation of the geochemical profiles ( $\epsilon\text{Nd}$  and  $\delta^{18}\text{O}_{\text{sw}}$ ) reveals contrasting trends during stadials and interstadials (Fig. 4). During the stadials, increase in the  $\epsilon\text{Nd}$  values (marked by arrows; Fig. 4) is observed during the enhanced precipitation phases (lower  $\delta^{18}\text{O}_{\text{sw}}$ ) which suggests a rise in the sediment contribution from the Brahmaputra sediment sources. Glacial expansion in the upper reaches of the Brahmaputra catchment dominated by THB (characterized by high  $\epsilon\text{Nd}$  values: Bikramaditya et al., 2020) during wet-stadials (Ray et al., 2015) possibly responsible for the observed  $\epsilon\text{Nd}$  trend. Expansion of Himalayan glaciers during wet-stadials has also been proposed by Owen et al, (2002). Enhanced sediment contribution by the THB rocks due to precipitation-induced glaciation (northern hemisphere glaciation) during the Plio-Pleistocene transition were reported by Galy et al, (2010) and Peketi et al, (2021). On the other hand, lower precipitation phases during the stadials do not show high  $\epsilon\text{Nd}$  values which may be attributed to reduced input from THB. The warm interstadials coupled with enhanced precipitation are accompanied by a shift towards lower  $\epsilon\text{Nd}$  values which may be attributed to extensive erosion of the Ganga catchment area comprising rocks characterized by lower  $\epsilon\text{Nd}$  values and diminished THB contribution due to lack of glacial erosion.

## Conclusion

The present study shows the predominance of the Himalayan sediments in the Mahanadi basin and this may be attributed to significantly higher sedimentation by the Ganga-Brahmaputra river system when compared to that of the Mahanadi river basin. The sedimentary sequence spanning 320 ky shows considerable temporal variations in the Sr-Nd isotope ratios. These temporal variations can be attributed to changes in the relative sediment contribution from Ganga and Brahmaputra rivers systems draining contrasting catchment lithologies with highly variable Sr-Nd isotope ratios. Here, we have emphasized the significance of glacial expansion and erosion of the THB rocks of Brahmaputra catchments during wet-stadials compared to dry-stadials. In contrast, the interstadials show enhanced precipitation and noticeable lower  $\epsilon_{\text{Nd}}$  values suggesting higher contribution of Ganga catchment with lower  $\epsilon_{\text{Nd}}$  values. This study signifies the importance of sediment provenance studies in the Indian peninsular basins for reconstructing the paleo climatic processes and organic matter source evaluation (Phillips et al., 2014; Da Silva et al., 2017; Mazumdar et al., 2015; Dunlea et al., 2020; Clemens et al., 2021).

## Funding information

This work was financially supported by the Ministry of Earth Sciences, Council of Scientific and Industrial Research, and Department of Science and Technology.

## CRedit author statement

**Aditya Peketi:** Conceptualization, Investigation, Methodology, Visualization, Formal analysis, Writing – original draft. **Aninda Mazumdar:** Conceptualization, Investigation, Methodology, Visualization, Funding acquisition, formal analysis, Writing – original draft. **S. Brahmanand:** Methodology. **SPK Pillutla:** Methodology. **Subhashree Mishra:** Methodology.

## Declaration of competing interest

The authors declare no conflict of interest.

## Acknowledgments

We acknowledge the Director, CSIR–NIO, and Secretary, MoES for supporting the gas hydrate program; National Gas Hydrate Program (NGHP) for scientific discussion, and background geology and ONGC for additional sites. We sincerely thank anonymous reviewers for their critical and meticulous review and valuable suggestions.

## References

- Ahmad, S.M., Padmakumari, V.M., Babu, G.A., 2009. Strontium and neodymium isotopic compositions in sediments from Godavari, Krishna and Pennar rivers. *Current science* 97, 1766-1769.
- Bastia, F., Equeenuddin, S.M., 2016. Spatio-temporal variation of water flow and sediment discharge in the Mahanadi River, India. *Global and Planetary Change* 144, 51-66.
- Bikramaditya, R.K., Chung, S.-L., Singh, A.K., Lee, H.-Y., Lin, T.-H., Iizuka, Y., 2020. Age and isotope geochemistry of magmatic rocks of the Lohit Plutonic Complex, eastern Himalaya: implications for the evolution of Transhimalayan arc magmatism. *Journal of the Geological Society* 177, 379-394.
- Chakrapani, G.J., Subramanian, V., 1990. Preliminary studies on the geochemistry of the Mahanadi river basin, India. *Chemical Geology* 81, 241-253.
- Clemens, S.C., Kuhnt, W., LeVay, L.J., Anand, P., Ando, T., Bartol, M., Bolton, C.T., Ding, X., Gariboldi, K., Giosan, L., 2015. International Ocean Discovery Program Expedition 353 preliminary report: Indian Monsoon Rainfall, 29 November 2014-29 January 2015.
- Clemens, S.C., Yamamoto, M., Thirumalai, K., Giosan, L., Richey, J.N., Nilsson-Kerr, K., Rosenthal, Y., Anand, P., McGrath, S.M., 2021. Remote and local drivers of Pleistocene South Asian summer monsoon precipitation: A test for future predictions. *Science Advances* 7, eabg3848.
- Clift, P.D., Giosan, L., Blusztajn, J., Campbell, I.H., Allen, C., Pringle, M., Tabrez, A.R., Danish, M., Rabbani, M.M., Alizai, A., 2008. Holocene erosion of the Lesser Himalaya triggered by intensified summer monsoon. *Geology* 36, 79-82.
- Da Silva, R., Mazumdar, A., Mapder, T., Peketi, A., Joshi, R.K., Shaji, A., Mahalakshmi, P., Sawant, B., Naik, B.G., Carvalho, M.A., 2017. Salinity stratification controlled productivity variation over 300 ky in the Bay of Bengal. *Scientific reports* 7, 1-7.
- Dangwal, V., Soma Sengupta, A.G.Desai, 2008. Speculated Petroleum Systems in Deep Offshore Mahanadi Basin in Bay of Bengal, India, 7th international conference & Exposition on petroleum Geophysics.
- Dunlea, A.G., Giosan, L., Huang, Y., 2020. Pliocene expansion of C4 vegetation in the core monsoon zone on the Indian Peninsula. *Clim. Past Discuss.* 2020, 1-17.
- Emmel, F.J., Curray, J.R., 1983. The Bengal submarine fan, northeastern Indian Ocean. *Geo-Marine Letters* 3, 119-124.
- France-Lanord, C., Derry, L., Michard, A., 1993. Evolution of the Himalaya since Miocene time: isotopic and sedimentological evidence from the Bengal Fan. *Geological Society, London, Special Publications* 74, 603-621.
- Garzanti, E., Ando, S., France-Lanord, C., Censi, P., Vignola, P., Galy, V., Lupker, M., 2011. Mineralogical and chemical variability of fluvial sediments 2. Suspended-load silt (Ganga-Brahmaputra, Bangladesh). *Earth Planet. Sci. Lett.* 302, 107-120, <http://dx.doi.org/10.1016/j.epsl.2010.11.043>.



- Galy, A., France-Lanord, C., Derry, L.A., 1999. The strontium isotopic budget of Himalayan rivers in Nepal and Bangladesh. *Geochimica et Cosmochimica Acta* 63, 1905-1925.
- Galy, V., France-Lanord, C., Peucker-Ehrenbrink, B., Huyghe, P., 2010. Sr-Nd-Os evidence for a stable erosion regime in the Himalaya during the past 12 Myr. *Earth and Planetary Science Letters* 290, 474-480.
- George, B.G., Ray, J.S., 2020. Depositional history of the Mesoproterozoic Chhattisgarh Basin, central India: insights from geochemical provenance of siliciclastic sediments. *International Geology Review* 63, 380-395.
- Goodbred, S.L., Paolo, P.M., Ullah, M.S., Pate, R.D., Khan, S.R., Kuehl, S.A., Singh, S.K., Rahaman, W., 2014. Piecing together the Ganges-Brahmaputra-Meghna River delta: Use of sediment provenance to reconstruct the history and interaction of multiple fluvial systems during Holocene delta evolution. *Geological Society of America Bulletin* 126, 1495-1510.
- Hein, C.J., Galy, V., Galy, A., France-Lanord, C., Kudrass, H., Schwenk, T., 2017. Post-glacial climate forcing of surface processes in the Ganges-Brahmaputra river basin and implications for carbon sequestration. *Earth and Planetary Science Letters* 478, 89-101.
- Jain, A.K., Banerjee, D.M., 2020. The Indian Subcontinent: Its Tectonics. *Proc Indian Natn Sci Acad* 86, 775-875.
- Lenard, S.J.P., Lave, J., France-Lanord, C., Aumaitre, G., Bourles, D.L., Keddadouche, K., 2020. Steady erosion rates in the Himalayas through late Cenozoic climatic changes. *Nature Geoscience*, 1-5.
- Lupker, M., France-Lanord, C., Galy, V., Lave, J., Kudrass, H., 2013. Increasing chemical weathering in the Himalayan system since the Last Glacial Maximum. *Earth and Planetary Science Letters* 365, 243-252.
- Mazumdar, A., Kocherla, M., Carvalho, M.A., Peketi, A., Joshi, R.K., Mahalaxmi, P., Joao, H.M., Jisha, R., 2015. Geochemical characterization of the Krishna-Godavari and Mahanadi offshore basin (Bay of Bengal) sediments: a comparative study of provenance. *Marine and Petroleum Geology* 60, 18-33.
- Meert, J.G., Pandit, M.K., Pradhan, V.R., Banks, J., Sirianni, R., Stroud, M., Newstead, B., Gifford, J., 2010. Precambrian crustal evolution of Peninsular India: a 3.0 billion year odyssey. *Journal of Asian Earth Sciences* 39, 483-515.
- Milliman, J.D., Syvitski, J.P.M., 1992. Geomorphic/tectonic control of sediment discharge to the ocean: the importance of small mountainous rivers. *The Journal of Geology* 100, 525-544.
- Owen, L.A., Finkel, R.C., Caffee, M.W., 2002. A note on the extent of glaciation throughout the Himalaya during the global Last Glacial Maximum. *Quaternary Science Reviews* 21, 147-157.
- Peketi, A., Mazumdar, A., Pillutla, S.P.K., Rai, V.K., Sawant, B., Chaitanya, A.V.S., 2020. Monsoon rainfall and contrasting source rocks influenced sediment composition of peninsular basins along the east coast of India (western Bay of Bengal). *Marine and Petroleum Geology* 118, 104433.

- Peketi, A., Mazumdar, A., Pillutla, S.P.K., Sawant, B., Gupta, H., 2021. Climatic and tectonic control on the Bengal Fan sedimentation since the Pliocene. *Geochemistry, Geophysics, Geosystems* 22, e2020GC009448.
- Phillips, S.C., Johnson, J.E., Giosan, L., Rose, K., 2014. Monsoon-influenced variation in productivity and lithogenic sediment flux since 110 ka in the offshore Mahanadi Basin, northern Bay of Bengal. *Marine and Petroleum Geology* 58, 502-525.
- Pierson-Wickmann, A.C., Reisberg, L., France-Lanord, C., Kudrass, H.R., 2001. Os-Sr-Nd results from sediments in the Bay of Bengal: Implications for sediment transport and the marine Os record. *Paleoceanography* 16, 435-444.
- Ramesh, R., Subramanian, V., 1988. Temporal, spatial and size variation in the sediment transport in the Krishna River basin, India. *Journal of Hydrology* 98, 53-65.
- Ray, P.A., Yang, Y.C.E., Wi, S., Khalil, A., Chatikavanij, V., Brown, C., 2015. Room for improvement: Hydroclimatic challenges to poverty-reducing development of the Brahmaputra River basin. *Environmental Science & Policy* 54, 64-80.
- Sastri, V., Venkatachala, B., Narayanan, V., 1981. The evolution of the east coast of India. *Palaeogeography, Palaeoclimatology, Palaeoecology* 36, 23-54.
- Singh, S.K., France-Lanord, C., 2002. Tracing the distribution of erosion in the Brahmaputra watershed from isotopic compositions of stream sediments. *Earth and Planetary Science Letters* 202, 645-662.
- Singh, M., Sharma, M., Tobschall, H.J., 2005. Weathering of the Ganga alluvial plain, northern India: implications from fluvial geochemistry of the Gomati River. *Applied Geochemistry* 20, 1-21.
- Singh, M., Singh, I.B., Muller, G., 2007. Sediment characteristics and transportation dynamics of the Ganga River. *Geomorphology* 86, 144-175.
- Singh, L., 2008. Oil and gas fields of India. Indian Petroleum Publishers, Dehradun.
- Singh, S.K., Rai, S.K., Krishnaswami, S., 2008. Sr and Nd isotopes in river sediments from the Ganga Basin: Sediment provenance and spatial variability in physical erosion. *Journal of Geophysical Research: Earth Surface* 113, F03006, doi:10.1029/2007JF000909.
- Singh, P., 2009. Major, trace and REE geochemistry of the Ganga River sediments: influence of provenance and sedimentary processes. *Chemical Geology* 266, 242-255.
- Subramanian, V., 1996. The sediment load of Indian rivers-an update. *IAHS Publications-Series of Proceedings and Reports-Intern Assoc Hydrological Sciences* 236, 183-190.
- Subramanian, V., Van't Dack, L., Van Grieken, R., 1985. Chemical composition of river sediments from the Indian sub-continent. *Chemical Geology* 48, 271-279.
- Subrahmanyam, V., Subrahmanyam, A.S., Murty, G.P.S., Murthy, K.S.R., 2008. Morphology and tectonics of Mahanadi Basin, northeastern continental margin of India from geophysical studies. *Marine Geology* 253, 63-72.

Tripathy, G.R., Singh, S.K., Bhushan, R., Ramaswamy, V., 2011. Sr-Nd isotope composition of the Bay of Bengal sediments: Impact of climate on erosion in the Himalaya. *Geochemical Journal* 45, 175-186.

Yin, A., 2006. Cenozoic tectonic evolution of the Himalayan orogen as constrained by along-strike variation of structural geometry, exhumation history, and foreland sedimentation. *Earth-Science Reviews* 76, 1-131.

## Figures and Table captions

**Figure-1:** Map showing core location (black star: MD161-19) along with other core locations (numerical 1-12) from upper, middle, lower Bengal fan (Emmel and Curray, 1983) and deeper waters of southern Mahanadi basin (Clemens et al., 2015) of which Sr-Nd isotope ratios were plotted along with the Sr-Nd isotope ratios of the present study. 1: KL105 (Lupker et al., 2013); 2: KL107 (Lupker et al., 2013); 3: KL117 (Lupker et al., 2013); 4: KL118 (Lupker et al., 2013); 5: U1445 (Peketi et al., 2021); 6: U1444 (Lenard et al., 2020); 7: U1454 (Lenard et al., 2020); 8: DSDP site 218 (Galy et al., 2010); 9: U 1450 (Lenard et al., 2020); 10: U1451 (Lenard et al., 2020); 11: Leg 717C (France-Lanord et al., 1993); 12: Leg 718C (France-Lanord et al., 1993). Sampling locations of Krishna, Godavari (Ahmad et al., 2009), and Mahanadi river (Numericals: 13-16; Peketi et al., 2021) bed sediments are also incorporated in the map. The map also shows Ganga, Brahmaputra, Krishna, Godavari, and Mahanadi river basins. Numericals from 17 to 39 represent the lithologies in the drainage basins of the Krishna (Ramesh and Subramanian, 1988), Godavari (Biksham and Subramanian, 1988), Mahanadi (Chakrapani and Subramanian, 1990), Ganga and Brahmaputra rivers (Yin et al., 2006; Jain and Banerjee, 2020). 17: Transhimalayan Batholith; 18: Indus-Tsangpo Suture Zone; 19: Tethyan Sedimentary Zone; 20: Higher Himalayan Crystalline Series; 21: Lesser Himalayas; 22: Siwalik Ranges along with Kirthar and Sulaiman Ranges; 23: Indo-Gangetic Brahmaputra Plain; 24: Delhi Sargodha Ridge; 25: Deccan Basalts; 26: Gondwana Supergroup; 27: Chotanagpur Granite Gneissic Complex; 28: Bogra Shelf; 29: Bengal Delta; 30: Proterozoic Sedimentary Basins; 31: Archean Tonalite-Trondjhemite Gneisses; 32: Khondalite Zone; 33: Migmatite Zone; 34: Paleoproterozoic Granite Enclaves; 35: Cenozoic-Holocene Sedimentary Cover; 36: Eastern Dharwar Craton; 37: Proterozoic Cuddapah-Kurnool Basin; 38: Nallamalai Fold Belt; 39: Nellore Greenstone Belt. Map modified after Peketi et al, (2021).

**Figure-2:** Sr and Nd isotope ratios mixing plot of the core MD161-19. The Sr-Nd isotope ratios of sediments from upper (Lupker et al., 2013), middle (Lupker et al., 2013), lower Bengal fan sediments (France-Lanord et al., 1993; Galy et al., 2010; Lenard et al., 2020) and Ganga & Brahmaputra main streams (Goodbred et al., 2014); Godavari, Krishna (Ahmad et al., 2009), Mahanadi river bed sediments (Peketi et al., 2021) are also incorporated. Numericals in the figure legend indicates the data locations mentioned in figure 1. Spread in the Sr-Nd isotope ratios of Transhimalayan Batholiths rocks is included as black rectangular box. Sr-Nd isotope ranges and mean values of source rocks (DcB: Deccan basalts; APGC: Archean Proterozoic Gneissic Complex; HHC: Higher Himalayan Crystalline Series; LH: Lower Himalayas) are used for mixing calculation. Average Sr and Nd concentrations and isotope ratios of the source rocks (Peketi et al., 2020) are: Deccan Basalts (224.34  $\mu\text{g/g}$ , 21.08  $\mu\text{g/g}$ ,

0.707113, -3.24), Archean Proterozoic gneissic complexes (377.85  $\mu\text{g/g}$ , 45.66  $\mu\text{g/g}$ , 0.760536, -30.72), Higher Himalayan Crystalline Series (80  $\mu\text{g/g}$ , 18  $\mu\text{g/g}$ , 0.76, -15) and Lesser Himalayas (94  $\mu\text{g/g}$ , 26  $\mu\text{g/g}$ , 0.85, -24.4).

**Figure-3:** Temporal profiles of MD161-19. (A)  $\delta^{18}\text{O}_{G.ruber}$  profile indicating marine isotope stages (MIS). MIS boundaries (1 to 9) are demarcated by dashed lines. MIS boundaries are demarcated as per Da Silva et al, (2017). (B)  $\epsilon\text{Nd}$  (C)  $^{87}\text{Sr}/^{86}\text{Sr}$  ratios. Red and green dashed lines in figure 3B, 3C indicate average Sr-Nd isotopic compositions of Ganga and Brahmaputra main stem averages respectively. Blue sections indicate stadial and orange sections indicate interstadial time periods.

**Figure-4:**  $\epsilon\text{Nd}$  of MD161-19 and salinity ( $\delta^{18}\text{O}$ ) profile of core U1446 (IODP-353 Clemens et al., 2021) for the last 320 ka. MIS boundaries are demarcated following figure 3.

**Figure-5:** Plot showing Fe/Al and  $\epsilon\text{Nd}$  values of MD161-9 along with average Fe/Al and  $\epsilon\text{Nd}$  values of Deccan Basalts and Archean Proterozoic Gneissic Complex source rocks (Mazumdar et al., 2015), Ganga and Brahmaputra river bed sediments (Goodberd et al., 2014).

**Figure-6:** Cross plot for mean grain size ( $D_{50}$ ) and  $^{87}\text{Sr}/^{86}\text{Sr}$  ratios of the MD161-19.

**Table 1:** Concentrations of Nd, Sr, Al, Fe,  $D_{50}$ , Fe/Al,  $^{87}\text{Sr}/^{86}\text{Sr}$  ratios &  $\epsilon\text{Nd}$  values of the core MD161-19.

Figure 1

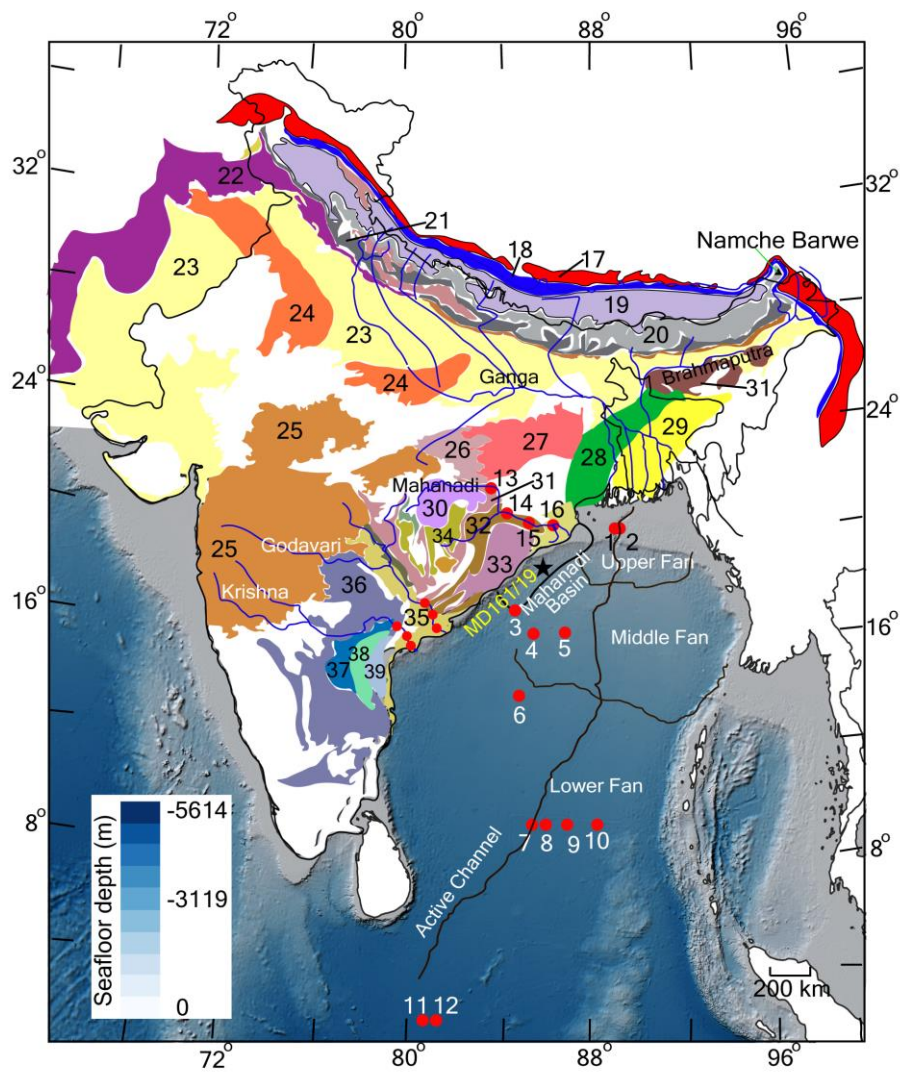
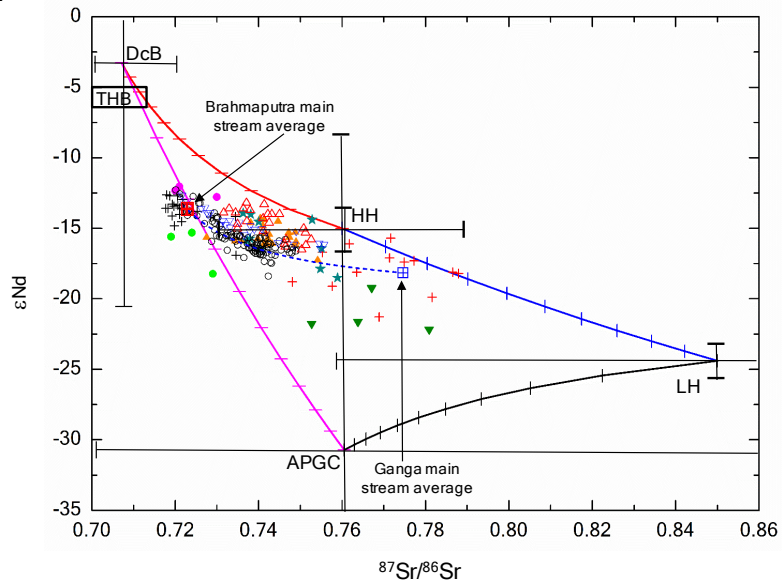


Figure 2



- + Brahmaputra river bed sediments
  - ▣ Brahmaputra main stem average
  - △ DSDP site 218 (8)
  - + Ganga river bed sediments
  - ▣ Ganga main stem average
  - Godavari river bed sediments
  - ★ Hole 717C (11), 718C (12)
  - ▲ KL105 (1), KL107 (2), KL117 (3), KL118 (4), KL120 (5)
- Krishna river bed sediments (Ahmad et al., 2009)
  - ▼ Mahanadi river bed sediments (Peketi et al., 2021)
  - MD161/19 (This study)
  - ▽ U 1444 (6), U1450 (9), U1451 (10), U1454 (7)

Figure 3

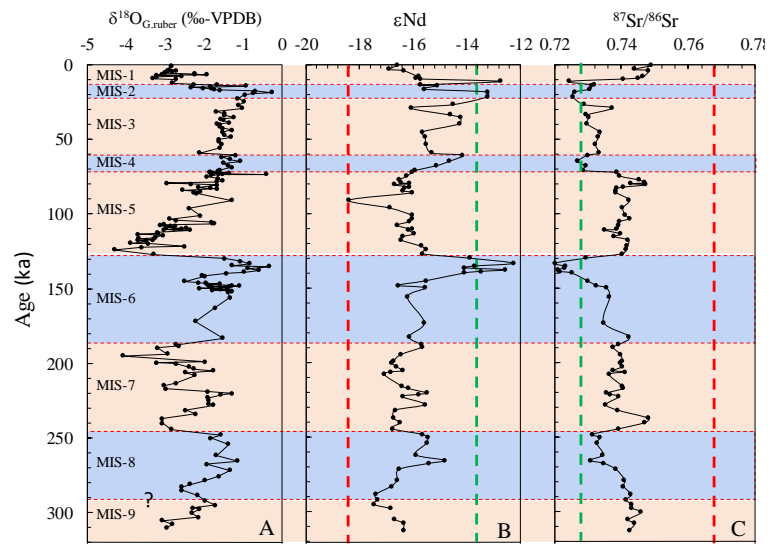




Figure 4

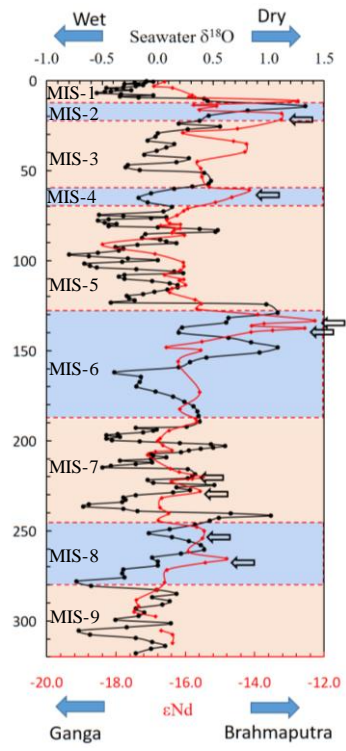


Figure 5

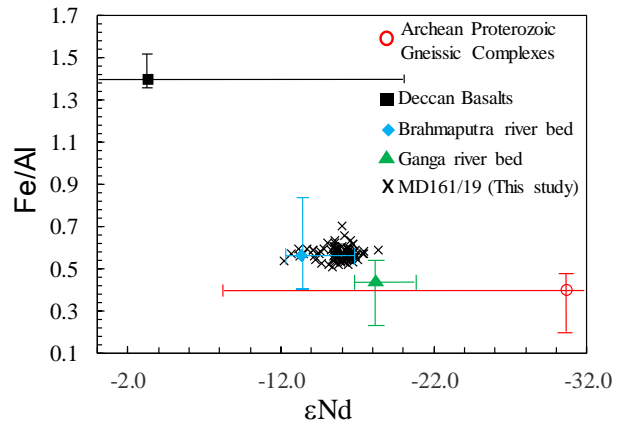
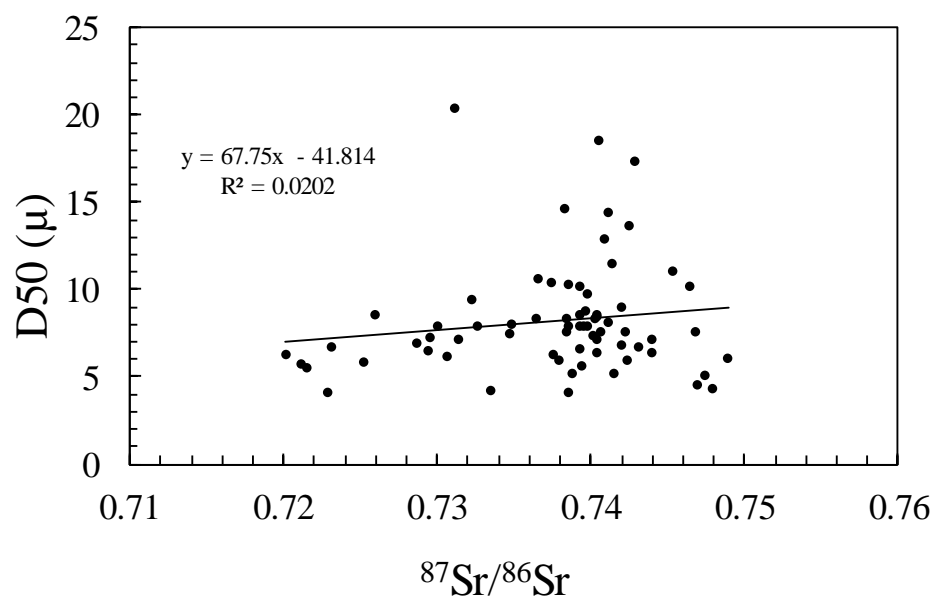


Figure 6



**Table 1**

SI . N o	Avg. Depth	Age	Nd	Sr	Fe	Al	Fe/A l	D5 0	<sup>143</sup> Nd/ <sup>144</sup> Nd	2 σ	εN d	<sup>87</sup> Sr/ <sup>86</sup> S r	2 σ
	(cmbs f)	(ky)	(ppm )	(ppm )	(% )	(% )		(μ)					
1	5	0.7	28.4	58.3	5.5	9.3	0.6	6.0	0.511787	1 0	- 16. 6	0.7489 3	9
2	168	3.2	33.3	91.6	5.5	10. 0	0.6	7.1	0.511771	1 2	- 16. 9	0.7439 5	8
3	198	4.1	30.5	73.9	5.6	9.8	0.6	4.3	0.511799	1 0	- 16. 4	0.7479 5	9
4	353	8.2						10. 1	0.511828	8	- 15. 8	0.7464 2	1 2
5	383	9.0	28.0	64.1	5.0	9.3	0.5		0.511823	1 5	- 15. 9	0.7449 4	1 5
6	405	9.6	30.4	78.7	5.1	9.2	0.6	6.3	0.511832	1 2	- 15. 7	0.7404 4	8

7	423	11.3	29.8	115.6	5.1	9.1	0.6		0.511985	1 0	- 12. 7	0.7243 1	1 5
8	448	13.6	26.9	77.4	5.2	8.8	0.6		0.511831	1 6	- 15. 7	0.7319 2	8
9	453	14.1	34.7	104.7	6.2	10. 0	0.6	20. 3	0.511864	8	- 15. 1	0.7311 7	1 2
10	478	16.5	36.7	114.7	5.9	10. 0	0.6		0.511839	1 2	- 15. 6	0.7306 3	9
11	498	18.3	28.3	92.4	5.1	8.6	0.6	8.4	0.511960	9	- 13. 2	0.7259 6	1 4
12	523	21.6	25.3	112.7	3.9	7.1	0.6		0.511959	1 0	- 13. 2	0.7256 2	1 0
13	558	26.8	37.5	123.2	5.3	9.3	0.6		0.511895	1 1	- 14. 5	0.7289 1	1 5
14	573	29.1	21.1	75.8	4.5	8.4	0.5		0.511813	1 5	- 16. 1	0.7372 8	1 2



23	863	65.0	27.5	106.4	4.0	7.8	0.5		0.511886	1 5	- 14. 7	0.7269 9	1 2
24	883	67.8	20.5	111.1	4.5	8.7	0.5		0.511862	9	- 15. 1	0.7294 4	1 0
25	905	71.0	30.0	102.7	4.4	8.3	0.5	6.9	0.511821	1 0	- 15. 9	0.7287 1	8
26	948	72.4	31.7	86.0	5.0	9.2	0.5	4.1	0.511815	1 5	- 16. 1	0.7384 9	1 2
27	1005	74.8	24.8		4.9	9.0	0.5	7.8	0.511805	9	- 16. 2	0.7395 5	1 0
28	1068	77.5	36.1	85.2	5.2	9.4	0.5	11. 0	0.511790	1 2	- 16. 5	0.7453 8	1 1
29	1108	79.2	28.9	67.9	4.8	8.0	0.6	4.5	0.511794	1 0	- 16. 5	0.7468 8	1 0
30	1128	79.9	30.7	77.0	5.0	9.3	0.5	17. 3	0.511811	1 8	- 16. 1	0.7428 5	9

31	1148	80.6	30.1	64.6	5.4	9.4	0.6	5.0	0.511781	1 2	- 16. 7	0.7473 8	8
32	1193	82.2	31.8	80.6	5.1	9.2	0.5	8.4	0.511811	1 0	- 16. 1	0.7404 4	1 2
33	1218	83.0	37.9	100.5	5.4	10. 0	0.5	10. 3	0.511801	9	- 16. 3	0.7386 0	1 0
34	1268	84.8	38.2	114.9	6.3	10. 9	0.6	14. 5	0.511798	1 4	- 16. 4	0.7383 2	8
35	1305	86.0	38.2	86.8	5.9	8.5	0.7	7.5	0.511816	8	- 16. 0	0.7384 5	9
36	1448	91.0	25.9	49.0	5.0	8.5	0.6		0.511695	8	- 18. 4	0.7423 3	1 1
37	1455	96.2	31.9	69.5	5.3	9.1	0.6	8.5	0.511773	9	- 16. 9	0.7403 9	8
38	1518	101. 0	35.7	90.8	5.4	9.5	0.6	14. 3	0.511815	9	- 16. 1	0.7411 2	1 0



39	1548	103. 3	29.4	69.8	5.3	9.4	0.6	13. 6	0.511815	1 2	- 16. 0	0.7424 4	8
40	1605	105. 3	40.0	90.1	4.9	8.6	0.6	5.6	0.511811	1 4	- 16. 1	0.7393 9	1 2
41	1673	107. 8	43.2	105.9	5.8	10. 4	0.6	7.8	0.511787	1 0	- 16. 6	0.7392 7	1 4
42	1748	110. 5	30.5	91.0	5.5	9.1	0.6	7.9	0.511815	9	- 16. 1	0.7385 3	1 6
43	1755	111. 0	33.6	89.2	4.9	9.0	0.6		0.511808	1 2	- 16. 2	0.7350 1	1 0
44	1793	113. 6	31.8	103.7	5.4	9.7	0.6	9.6	0.511818	1 0	- 16. 0	0.7397 2	8
45	1818	115. 4	39.5	108.5	5.4	9.6	0.6	5.9	0.511798	1 5	- 16. 4	0.7378 7	9
46	1848	117. 6	31.1	76.1	5.1	9.2	0.6	8.9	0.511794	1 6	- 16. 5	0.7419 8	1 0

47	1905	121. 8	36.6	82.8	5.0	8.7	0.6		0.511833	8	- 15. 7	0.7416 8	8
48	1943	123. 8	33.0	88.0	5.5	9.8	0.6	5.1	0.511842	9	- 15. 5	0.7414 9	1 3
49	1973	126. 9	30.0	84.8	5.5	9.1	0.6	8.3	0.511835	1 0	- 15. 7	0.7402 4	1 3
50	2003	129. 8						6.4	0.511925	1 2	- 13. 9	0.7293 9	1 0
51	2055	133. 3	28.2	153.0	3.2	6.0	0.5	6.1	0.512009	8	- 12. 3	0.7201 2	8
52	2083	135. 1	29.6	145.2	5.4	9.1	0.6	6.6	0.511935	1 0	- 13. 7	0.7231 7	9
53	2118	136. 3	26.8	153.0				4.0	0.511916	1 2	- 14. 1	0.7229 2	1 5
54	2153	137. 6		86.1				5.6	0.511994	9	- 12. 6	0.7211 1	1 0

55	2183	138. 7	27.9	171.1	5.1	9.0	0.6	5.4	0.511947	1 1	- 13. 5	0.7215 1	8
56	2213	139. 8	29.1	145.9	5.1	8.8	0.6	5.7	0.511915	9	- 14. 1	0.7251 9	9
57	2268	145. 0	34.4	106.4	5.7	9.3	0.6		0.511842	1 0	- 15. 5	0.7299 0	1 2
58	2303	148. 1	32.7	112.4	5.9	9.3	0.6		0.511789	9	- 16. 6	0.7325 1	9
59	2323	149. 8	23.2	70.0	5.6	8.9	0.6		0.511840	1 2	- 15. 6	0.7355 5	8
60	2393	156. 0	32.2	98.3	6.0	9.1	0.7	8.2	0.511807	1 4	- 16. 2	0.7364 9	1 2
61	2448	173. 1	35.9	123.0	5.2	9.7	0.5	7.4	0.511839	1 2	- 15. 6	0.7347 2	8
62	2478	182. 4	34.4	101.1	5.4	10. 2	0.5	7.5	0.511810	1 0	- 16. 2	0.7422 7	9

63	2513	187. 7	34.5	100.0	5.7	10. 1	0.6	8.4	0.511833	8	- 15. 7	0.7392 3	1 6
64	2528	189. 6	37.7	105.6	5.6	10. 1	0.5	10. 4	0.511834	9	- 15. 7	0.7374 4	9
65	2568	194. 5	34.8	103.3	5.3	9.6	0.6	7.8	0.511794	7	- 16. 5	0.7397 2	1 0
66	2603	198. 9	39.4	96.3	5.9	9.6	0.6	7.2	0.511780	1 2	- 16. 7	0.7401 8	8
67	2613	200. 1	38.3	104.8	5.7	10. 3	0.6	8.7	0.511777	9	- 16. 8	0.7396 9	1 2
68	2633	202. 6	35.2	82.9	5.1	8.8	0.6	7.1	0.511785	1 1	- 16. 6	0.7403 4	1 4
69	2655	205. 3	33.7	89.0	4.1	7.9	0.5	6.1	0.511798	1 3	- 16. 4	0.7375 9	1 1
70	2683	206. 2	37.9	99.3	5.5	10. 0	0.5	8.0	0.511774	8	- 16. 9	0.7411 3	8

71	2718	208. 0	36.6	121.3	5.5	10. 2	0.5		0.511762	9	- 17. 1	0.7364 5	9
72	2863	215. 5	33.1	99.4	5.7	10. 1	0.6		0.511795	8	- 16. 4	0.7401 5	8
73	2898	217. 3	32.6	58.0	5.1	8.7	0.6	18. 4	0.511808	1 2	- 16. 2	0.7405 3	7
74	2955	220. 3	30.5	79.3	4.8	8.7	0.6		0.511844	8	- 15. 5	0.7356 3	1 2
75	2973	221. 2	29.9	76.6	4.6	8.9	0.5	10. 5	0.511828	9	- 15. 8	0.7366 0	1 4
76	3003	222. 8	40.0	94.4	5.6	9.9	0.6	10. 1	0.511797	1 1	- 16. 4	0.7392 5	1 5
77	3068	228. 0	33.9	114.3	5.0	9.5	0.5		0.511840	1 2	- 15. 6	0.7354 0	9
78	3105	231. 8	31.7	93.5	5.1	9.4	0.5	5.2	0.511783	1 4	- 16. 7	0.7387 7	1 1

79	3158	237. 2	32.1	90.8	5.1	9.6	0.5		0.511780	1 0	- 16. 7	0.7479 5	1 4
80	3188	240. 2	34.9	83.7	5.4	10. 1	0.5	7.5	0.511793	1 3	- 16. 5	0.7468 4	1 0
81	3223	244. 3						6.5	0.511778	8	- 16. 8	0.7392 5	1 1
82	3255	248. 0	28.5	87.6	4.7	8.0	0.6	7.0	0.511834	9	- 15. 7	0.7313 5	8
83	3273	250. 1	21.8	79.7	3.3	6.0	0.5		0.511845	9	- 15. 5	0.7335 8	9
84	3308	254. 2	30.6	108.7	5.4	9.0	0.6	7.8	0.511843	1 2	- 15. 5	0.7326 4	1 0
85	3373	261. 7	29.2	86.5	4.3	8.1	0.5		0.511822	1 6	- 15. 9	0.7345 2	1 4
86	3405	265. 4	24.7	85.0	4.7	8.0	0.6	6.1	0.511879	1 2	- 14. 8	0.7307 0	1 0

87	3423	267. 5	26.2	86.2	3.8	7.5	0.5	8.0	0.511847	1 1	- 15. 4	0.7348 5	8
88	3458	271. 6	38.4	101.8	5.3	9.9	0.5	8.3	0.511790	8	- 16. 5	0.7383 7	1 1
89	3518	278. 6	36.6	91.4	5.6	9.9	0.6	12. 8	0.511787	1 2	- 16. 6	0.7409 3	1 2
90	3555	282. 9	29.0	66.6	5.2	9.0	0.6	7.5	0.511775	9	- 16. 8	0.7406 3	9
91	3608	288. 5	31.8	88.0	6.0	10. 3	0.6		0.511745	1 2	- 17. 4	0.7428 6	1 2
92	3643	292. 0	37.5	103.3	5.7	10. 1	0.6	11. 4	0.511749	1 0	- 17. 3	0.7413 3	1 3
93	3673	295. 0	33.8	72.3	4.7	8.3	0.6		0.511742	1 0	- 17. 5	0.7431 2	8
94	3705	297. 6	31.5	74.6	5.2	9.3	0.6	6.6	0.511774	9	- 16. 9	0.7431 4	1 4

95	3738	300. 4	34.3	85.1	5.6	9.8	0.6					0.7458 7	8
96	3798	305. 3	30.3	69.1	5.6	9.2	0.6	6.7	0.511782	8	- 16. 7	0.7420 2	8
97	3828	307. 8	18.3	52.1	5.3	8.9	0.6	6.3	0.511799	1 5	- 16. 4	0.7439 5	9
98	3883	312. 3	28.1	76.8	5.7	9.6	0.6	5.9	0.511799	1 2	- 16. 4	0.7424 1	1 1